Proceedings Paper:
Pan, X, Huang, H and Zhang, L (2020) Power Flow Control using a Bidirectional Z-source Inverter–based Static Synchronous Series Compensator. In: Proceedings of the 2020 22nd European Conference on Power Electronics and Applications (EPE'20 ECCE Europe). 2020 22nd European Conference on Power Electronics and Applications (EPE'20 ECCE Europe), 07-11 Sep 2020, Online. ISBN: 978-1-7281-9807-1. ISSN: 2693-4949.

https://doi.org/10.23919/EPE20ECCEEurope43536.2020.9215650

Power Flow Control using a Bidirectional Z-source Inverter–based Static Synchronous Series Compensator

Xuejiao Pan, Han Huang, Li Zhang
School of Electronic and Electrical Engineering, University of Leeds, Leeds, UK
Tel.: +44 7306314840
E-Mail: ml16xp@leeds.ac.uk
URL: http://www.leeds.ac.uk

Keywords:

«Z-source converter», «FACTS», «Predictive control», «Power transmission»

Abstract

The Static Synchronous Series Compensator, performing power control and reactive power compensation, is an important aid to stable and flexible operation of recent electrical power distribution networks. The paper describes a compensator based on a bidirectional Z-source inverter with PWM technology. This inverter has a wide control range and does not require a switching dead time. Its design using small signal theory to obtain suitable L-C network parameters for desired time response is described. Model predictive current control and direct current control schemes are analysed and compared, and satisfactory performance of the whole compensator is demonstrated.

Introduction

With increasing penetration of renewable sourced generation into the power network, an emerging trend in the electricity supply industry is a shift from large power plant to small distributed generation (DG) systems located near the point of consumption and forming a microgrid. Apart from the clear benefit of decarbonisation, such a trend reduces reliance on long, heavily loaded lines, with their associated losses. However it also brings considerable challenges; the unpredictable nature of the renewable energy sources introduces more modes of power flow in the system and the capacity of some existing transmission lines can become overloaded. Also having increasing numbers of DGs, the whole power network structure becomes more complex, its stability margin may be narrowed and its robustness may be reduced.

The Static Synchronous Series Compensator(SSSC), as one of the Flexible AC Transmission system (FACTS)[1,2] is effective in controlling power flow, and hence can reduce power flow in heavily loaded lines and can support voltages by controlling effective line series impedance, and improve the stability of the network. Most SSSCs use an H-bridge based voltage source converter (VSC) to inject a controllable voltage in series with the transmission line where it is connected. By flexibly regulating its voltage magnitude and phase angle it provides both capacitive and inductive impedance compensation independent of the power line current, or real and reactive power flow regulation. However the output voltage of the conventional VSC

is always lower than its dc input voltage, which may restrict its compensation range. Although adding a DC-DC converter can boost the input voltage, it adds complexity in the circuit structure and control scheme. There is also the possible danger of a DC-side circuit current surge due to turning on two switching devices in the same phase limb simultaneously. A switch blanking time is always inserted to prevent the danger but this brings output waveform distortion.

This paper presents a bidirectional z-source inverter (ZSI)-based SSSC for the active and reactive power flow control of a power line. The device, proposed originally by Fang zheng Peng *et al* [3,4], combines a z-source DC-DC converter which allows current flow in and out of DC source and an H-bridge DC-AC inverter. With the fixed input voltage it can buck or boost the output AC voltage and can also perform four-quadrant operation. A special feature of the ZSI is that two switches in one phase limb of the H-bridge can be closed simultaneously for performing the same function as the shoot-through state of a z-source dc-dc converter. Unlike the conventional z-source inverter, the bidirectional feature of this converter enables energy exchange between AC and DC sides in both directions. Also, the BZSI is able to completely avoid the undesirable operation modes when the ZSI operated under a small inductance or a low load power factor. The paper will show the effectiveness of this SSSC in regulating the power flow by adjusting the line impedance can be comparable to its conventional VSC-based counterpart.

In the paper two different control schemes are described and their performances are compared for this BZSI-SSSC; one is direct power control and the other is model predictive control. Results show that both can result in the BZSI-SSSC injecting the desired voltage to the transmission line.

Configuration of the Power System with a BZSI-SSSC

The configuration of the power system studied with a BZSI as an SSSC is shown in Fig. 1. There are two buses; the sending bus is represented by a 3-phase voltage source supplying a transmission line with impedance $R_S + jX_S$. The receiving bus has two R-L loads of different power ratings connected, and a generator, supplying power demand locally, represented by a a voltage source with impedance $R_R + jX_R$. The BZSI-SSSC is connected serially in the transmission lines through a three phase transformer near the receiving bus, also called the point of common connection (PCC).

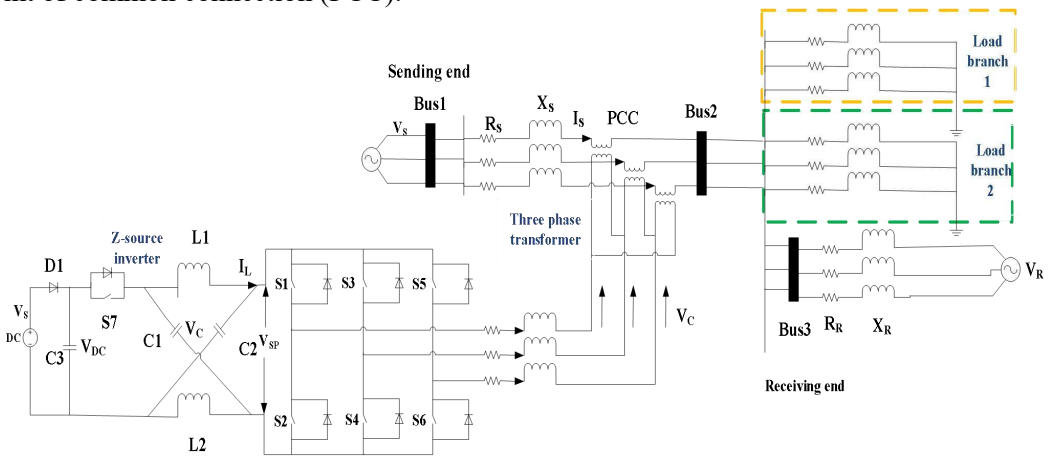

Fig. 1 Configuration of the system controlled by a ZSI-based SSSC

BZSI Operation Modes and Parameter Selection

This topology, as shown in Fig.2, can overcome the shortcomings of the traditional ZSI by shunting the DC side diode D_1 with a switch S_7, which enables bidirectional input current, and hence allows DC and AC side energy exchange.

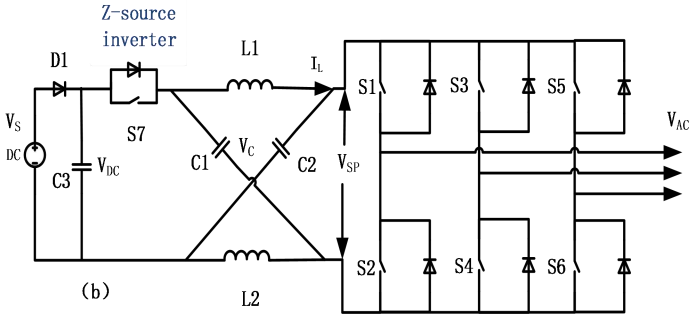

Fig.2 Topology of bi-directional z-source inverter

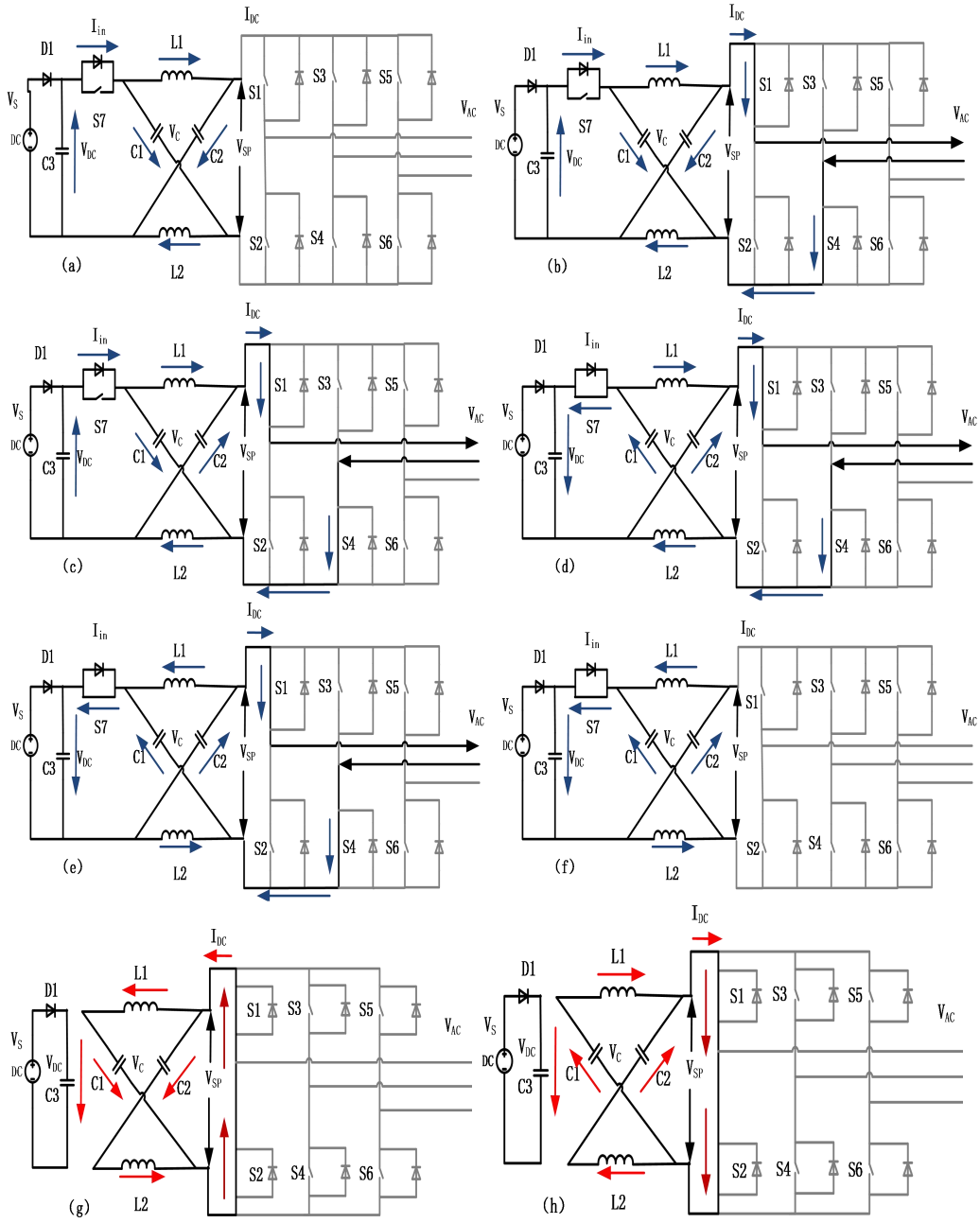

Fig.3 Eight operation modes for a BZSI

Operation Modes

The basic operation comprises just active and shoot-through modes; however in view of the alternative current path, there can be eight working modes within one switching cycle.

Mode a: The input diode D_1 conducts and the switch S_7 is open,. no switches in the H-bridge are on, so there is no current flowing into the AC load side, I_{DC}=0. The DC-side capacitor C_3 charges the Z-network capacitors C_1 and C_2 together with L_1 and L_2.

Mode b: D_1 remains on, H-bridge is active, hence load current, I_{DC} is flowing to the AC side. Z-network capacitors C_1 and C_2 are still in charging mode. The input DC current I_{in} is positive and inductor current I_L discharges to the inverter and satisfies the following relationship:

$$I_L > I_{DC}/2 \tag{1}$$

Mode c: As I_L continues to flow to the load side and is decreasing, C_1 discharges to load, and C_2 is in charge mode, I_{in} is still positive.

Mode d: As I_L decreases to a half of the output current I_{DC}, switch S_7 is turned on I_{in} becomes negative. The current relationship is shown in below:

$$I_{in} < 0,\ 0 < I_L < I_{DC}/2 \tag{2}$$

Mode e: Inductor current drops below 0, S_7 is still on. Z-network capacitors C_1 and C_2 discharge and input side capacitor C_3 is charged.

$$I_{in} < 0, I_L < 0 \tag{3}$$

Mode f: H-bridge is inactive, I_{DC}=0, Z-network is isolated from H bridge. S_7 is still on. Input and inductor currents are all negative.

Mode g: H-bridge inverter is in shoot through mode. The sum of capacitor voltages (V_{C1}+V_{C2}) is larger than the DC source voltage V_S. Switch S_7 and diode are off. The Z-network capacitors are charging the inductors.

Mode h: After negative inductor current reduces to 0, the arm is shorted by the shoot-through signal. The output voltage V_{AC} is 0.

In summary, modes b to e are active modes and modes g, h are shoot through modes. Meantime, there are two non-shoot through zero states which are modes a and f. When inductor current I_L falls below $I_{DC}/2$ and even become negative (modes d and e), C_1 and C_2 discharge and switch S_7 is on so that current can flow back to DC side capacitor C_3.

Transfer Function Derivation and BZSI design

The transient characteristic of a BZSI depends on its inductor and capacitor values. Their selection can be based on the frequency and time domain analysis using the small signal transfer function between the capacitor voltage and the shoot-through duty ratio derived as follows.

Assuming the load impedance is R_L +jX_L and I_{DC} is the output DC current. With the switching period setting as T sec. and shoot-through time ratio D, the time duration for active mode is (1-D)T and shoot through mode is DT. By setting the state variables $x = [I_{L1} \quad I_{L2} \quad V_{C1} \quad V_{C2} \quad I_{DC}]^T$ and the input $u = V_{DC}$, the state-space average equation combining both switch turn-on and off for continuous-conduction mode is given as[4]:

$$\begin{bmatrix} \frac{dI_{L1}}{dt} \\ \frac{dI_{L2}}{dt} \\ \frac{dV_{C1}}{dt} \\ \frac{dV_{C2}}{dt} \\ \frac{dI_{L_L}}{dt} \end{bmatrix} = \begin{bmatrix} 0 & 0 & DT/L & -(1-D)T/L & 0 \\ 0 & 0 & -(1-D)T/L & DT/L & 0 \\ -DT/C & (1-D)T/C & 0 & 0 & -(1-D)T/C \\ (1-D)T/C & -DT/C & 0 & 0 & -(1-D)T/C \\ 0 & 0 & (1\text{-}D)T/L_L & (1\text{-}D)T/L_L & -R_L/L_L \end{bmatrix} \begin{bmatrix} I_{L1} \\ I_{L2} \\ V_{C1} \\ V_{C2} \\ I_{DC} \end{bmatrix} + \begin{bmatrix} (1-D)T/L \\ (1-D)T/L \\ 0 \\ 0 \\ -(1-D)T/L \end{bmatrix} V_{DC} \tag{4}$$

The above can be written as $\frac{dx}{dt} = Ax + Bu$ and is zero at the steady state, hence leads to capacitor voltages and inductor currents given as:

$$V_{C1} = V_{C2} = \frac{1-D}{1-2D} V_{DC} \tag{5}$$

The relationship between output DC voltage V_{SP} and input V_{DC} is expressed as:

$$\frac{V_{SP}}{V_{DC}} = \frac{1}{1-2D} \tag{6}$$

Connecting a DC-AC inverter with amplitude modulation index M_a, at the output DC-line the ratio of V_{AC} to V_{DC} can be expressed as:

$$\frac{V_{AC}}{V_{DC}} = \frac{M_a}{1-2D} \tag{7}$$

For the DC-AC inverter, since modulation index Ma ranges from 0 to 1, the AC-side voltage magnitude V_{AC} can be lower than the DC-bus voltage V_{SP}. However according to Equation (6), the DC-output voltage changes from positive to negative according to D; for $0 < D < 0.5$, it varies from 1 to $+\infty$ and for $0.5 < D < 1$ it is negative varying from $-\infty$ to -1. Consequently V_{AC} can be boosted or bucked relative to the input DC voltage V_{DC}, and is bidirectional thus giving more flexibility in voltage control.

Introducing small perturbation to shoot through duty ratio in Equ (4), the small perturbations in the capacitor voltage and inductor current $\hat{v}_C(t), \hat{i}_L(t)$ can be obtained. Taking Laplace transform, their s-domain expressions corresponding to $\hat{d}(t)$ are expressed as :

$$\hat{v}_c(s) = \frac{a_1 S^2 + a_2 S + a_3}{b_3 S^3 + b_2 S^2 + b_1 S + b_0} \hat{d}(s) \tag{9}$$

The corresponding coefficients a_1 to a_6 and b_0 to b_3 are listed in Appendix. Subsequently the transfer function between $\hat{v}_C(t)$ and $\hat{d}(t)$ is obtained as:

$$G_{cd} = \frac{\hat{v}_c(s)}{\hat{d}(s)} = \frac{a_1 S^2 + a_2 S + a_3}{b_3 S^3 + b_2 S^2 + b_1 S + b_0} \tag{10}$$

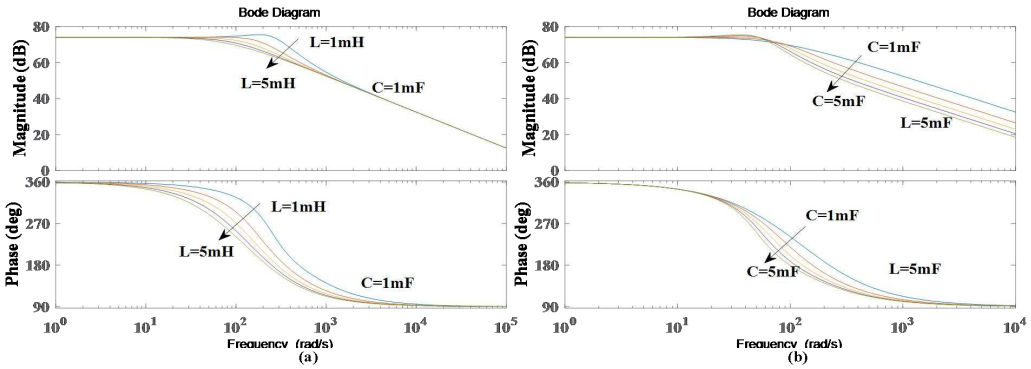

Fig.4 Bode plots $\hat{v}_C(s)/\hat{d}(s)$ for:(a) inductance changing with constant capacitance; (b)capacitance changing with constant inductance

The Bode plots and step response diagrams of this transfer function for the inductor value varying from 1mH to 5mH and capacitor value changing from 1mF to 5mF are as shown in Fig.4 and Fig.5 and they all present under-damped characteristics. It can be seen in Fig.4 that increasing inductance value leads to the reduction of gain values. However, as capacitance increases, gain value increases. Lower gain amplitude gives lower oscillation, but larger inductor. So L =5mH and C= 1mF are chosen. In Fig.5, the response curve having L =5mH and C= 1mF gives the lowest level of overshoot with the shortest transient response time, so these two parameter values are chosen.

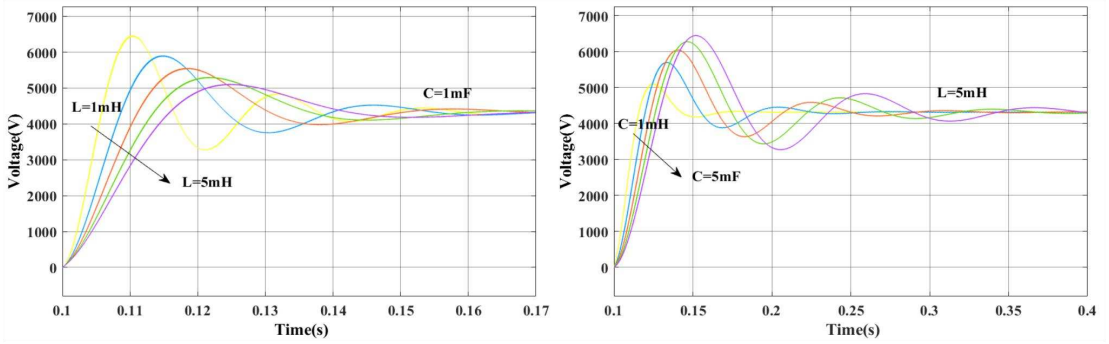

Fig.5 Step response diagrams:(a)inductance changing with constant capacitance; (b)capacitance changing with constant inductance

Control Schemes

The control strategy for SSSC consists of two parts; AC control for regulating the magnitude and phase angle of line inserted voltage V_C, and DC control for maintaining V_{sp} at a required level. The objective of the SSSC control is to ensure that the real and reactive powers flowing along the transmission line between the sending and receiving ends are at the required levels. Taking the sending end voltage as the reference, and using a d-q synchronous reference frame the reference real and reactive power values P_{ref} and Q_{ref} at the sending end can be calculated, respectively, as

$$P_{ref} = \frac{3}{2} V_S \times I_S \times \cos(\theta_i) = \frac{3}{2} V_S \times I_d \tag{11}$$

$$Q_{ref} = -\frac{3}{2} V_S \times I_S \times \sin(\theta_i) = -\frac{3}{2} V_S \times I_q \tag{12}$$

where θ_i is the phase angle between sending end voltage V_S and sending end current I_S.

Power Flow Control

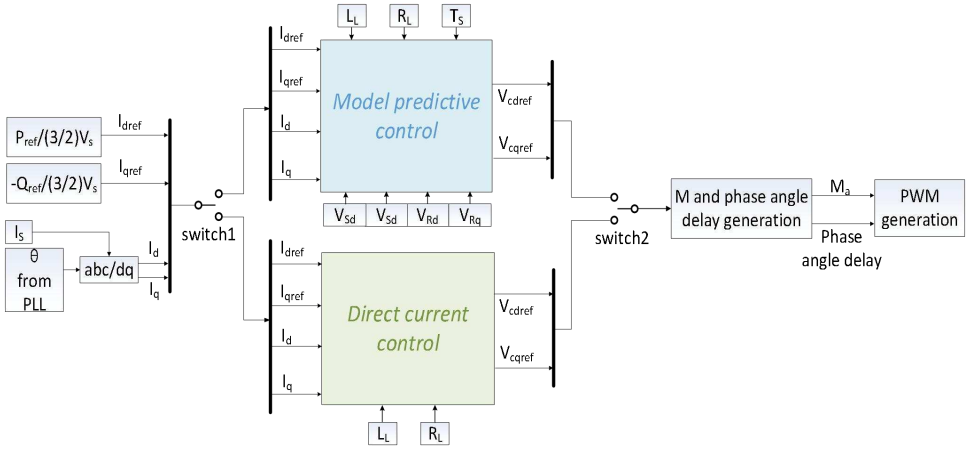

Fig. 6 Schematics of the Model predictive current control and direct current control schemes

For AC control part, With the desired P_{ref} and Q_{ref}, and measured sending end voltage V_S, the reference current I_{dref} and I_{qref} can be calculated from equations (11) and (12); using the line impedance $R_L + jX_L = (R_S+R_R)+j(X_S+X_R)$. The amplitude and phase of the desired compensation voltage can be calculated as the target and realised by different current control methods of which two are described below and shown in Fig. 6.

Model Predictive Current Control

In this control scheme the required compensation voltage from BZSI-based SSSC terminals is derived through the equation(13)[7,8,9].

$$\vec{V}_{Cref}(K)=\vec{V}_S(K)-\vec{V}_R(K)-L_L\frac{d\vec{I}_S(K)}{dt}-R_L\vec{I}_S(K)=\vec{V}_S(K)-\vec{V}_R(K)-L_L\frac{\vec{I}_S(K+1)-\vec{I}_S(K)}{T_s}-R_L\vec{I}_S(K) \quad (13)$$

Because the value of current $I_S(K+1)$ at the next sampling time cannot be measured in advance, the reference current I_{sref} is used to replace its role. Thus the equation can be expressed in (14), while its dq form is shown as (15).

$$\vec{V}_{Cref}(K)=\vec{V}_S(K)-\vec{V}_R(K)-\left[\frac{L_L}{T_S}\right]\vec{I}_{Sref}(K)+\left[\frac{L_L}{T_S}-R_L\right]\vec{I}_S(K) \quad (14)$$

$$\begin{bmatrix}\vec{V}_{Cdref}(K)\\ \vec{V}_{Cqref}(K)\end{bmatrix}=\begin{bmatrix}\vec{V}_{Sd}(K)\\ \vec{V}_{Sq}(K)\end{bmatrix}-\begin{bmatrix}\vec{V}_{Rd}(K)\\ \vec{V}_{Rq}(K)\end{bmatrix}-\begin{bmatrix}\frac{L_L}{T_S} & 0\\ 0 & \frac{L_L}{T_S}\end{bmatrix}\begin{bmatrix}\vec{I}_{sdref}(K)\\ \vec{I}_{sqref}(K)\end{bmatrix}+\begin{bmatrix}\frac{L_L}{T_S}-R_L & -\omega L_L\\ \omega L_L & \frac{L_L}{T_S}-R_L\end{bmatrix}\begin{bmatrix}\vec{I}_{sd}(K)\\ \vec{I}_{sq}(K)\end{bmatrix} \quad (15)$$

By using reference angle θ which is from the phase locked loop(PLL) and ABC-dq block, measured currents I_d and I_q in dq form are obtained. The reference currents I_{dref} and I_{qref} can be calculated by equations (11) and (12). The magnitude and phase angle of the required compensation voltage can be realized by modulation index M_a and angle delay.

Direct Current Control

The voltage difference between the sending and receiving terminals can be expressed as

$$\begin{aligned}\Delta V &= V_C = V_S - V_R(\cos\theta_R + j\sin\theta_R)\\ &= V_C(\cos\theta_C - j\sin\theta_C)+(R_L+jX_L)I(\cos\theta_i+j\sin\theta_i)\end{aligned} \quad (16)$$

where θ_R is the phase angle of V_R with respect to V_S, θ_i is the current phase angle compared to V_S, θ_C is the phase angle between the injected compensating voltage and V_S. Expressing ΔV in d-q form, these two elements are given by

$$\begin{aligned}V_{Cdref} &= V_S - V_R\times\cos\theta_R - R_L I\times\cos\theta_i + X_L I\times\sin\theta_i\\ &= \Delta V_d - R_L I_d + X_L I_q = (K_p+\frac{K_i}{s})(I_{dref}-I_d)-R_L I_d+\omega L I_q\\ V_{Cqref} &= -V_R\times\sin\theta_R - R_L I\times\sin\theta_i - X_L I\times\cos\theta_i\\ &= \Delta V_q - R_L I_q - X_L I_d = (K_p+\frac{K_i}{s})(I_{qref}-I_q)-R_L I_q-\omega L I_d\end{aligned} \quad (17)$$

The reference current I_{dref} and I_{qref} calculated from equations (11) and (12) are compared with the real currents I_d and I_q and the error are used to track ΔV through PI controller. Through equation (17), reference compensated voltage V_{Cdref} and V_{Cqref} can be calculated.

DC Voltage Control

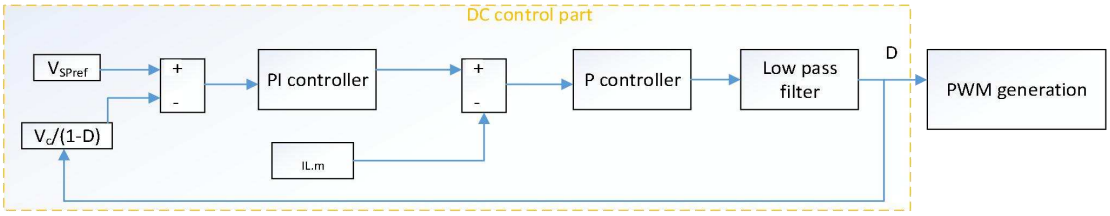

Fig.7 Block diagram of DC control scheme

For DC control shown in Fig.7, reference output DC voltage V_{SPref} needs to be set higher than compensated voltage V_C. Since M_a is in the range between 0 and 1. The DC-side output voltage V_{SP} is equal to V_C/ (1-D) which allows determination of the factor D, noting that V_C is the measured capacitor voltage as shown in Fig.1. In this case, DC supply side provide DC voltage 2KV and output DC voltage V_{SP} need to be kept at 10KV so that shoot through duty ratio D should be maintained at 0.4.

Pulse Width Modulation (PWM)

There are three control methods[6] can be used to generate PWM pulse signals to control switches in the H bridge, namely simple boost control(SBC), maximum boost control(MBC) and maximum constant boost control(MCBC).Considering the special nature of control strategy which is shown in above, shoot through duty ratio D and modulation index M_a should be controlled separately. So simple boost control is chosen. This employs the basic three-phase sine-triangle PWM scheme and also uses a positive and a negative reference levels with magnitudes equal to the amplitude of the sinusoidal reference signal to intersect the triangular carrier wave.

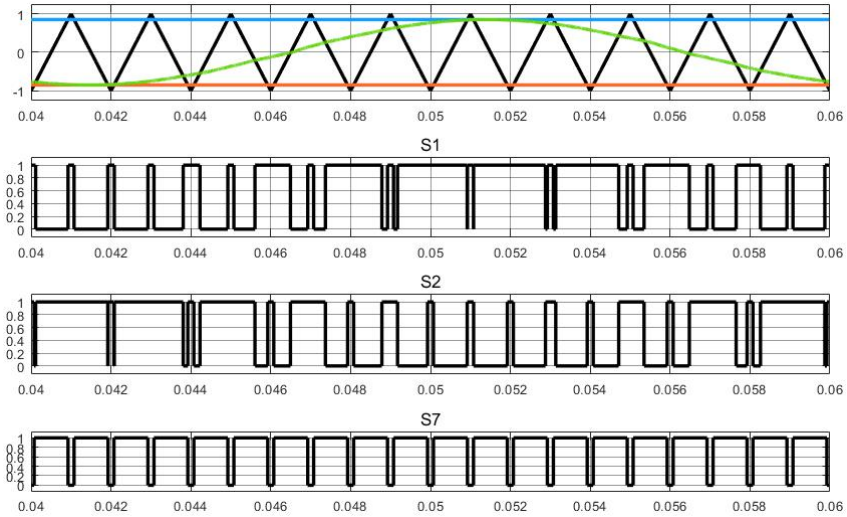

Fig.8 PWM signals using SBC for two switches in phase A and input side switch S7

As shown in Fig.8, the blue and red lines are positive and negative reference levels which are determined by shoot through duty ratio D and the magnitude is equal to 1-D. The green curve represents phase A of output voltage V_{AC}, and the magnitude is modulation index M_a. After comparing with the carrier wave, control signals for S1 and S2 are generated. According to the working modes in Fig.3, the control signal of switch S7 satisfies that it is complementary to the shoot through signal for bidirectional ZSI. The remaining four switches S3, S4, S5, and S6 are controlled using sinusoidal signals of phases B and C.

Simulation Results

To validate the above control scheme, simulation studies were performed using all parameters listed in the table below. The whole system can be translated into the per unit(pu) system when the base power S_{base} and base voltage V_{base} are chosen.

Table I:Parameter of model

DC input voltage V_{DC}	2000V
Base power S_{base}	10MW
Base voltage(rms , phase-ground)	11kV
Inductors L_1 and L_2 in BZSI	2mH
Capacitors C_1 and C_2 in BZSI	1mF
Transformer ratio	1:1
Resistance in transmission line R_S and R_R	0.065Ω/km
Inductance in transmission line X_S and X_R	0.0844mH/km
Length of transmission line	50km
Sending terminal voltage V_S(rms , phase-ground)	$11\angle 0°$ kV

Receiving terminal voltage V_R(rms , phase-ground)	11∠15° kV
Real power for each load branch	0.5 MW
Reactive power for each load branch	-0.5 MW
Switching frequency	20 kHz

Simulation results for different control methods

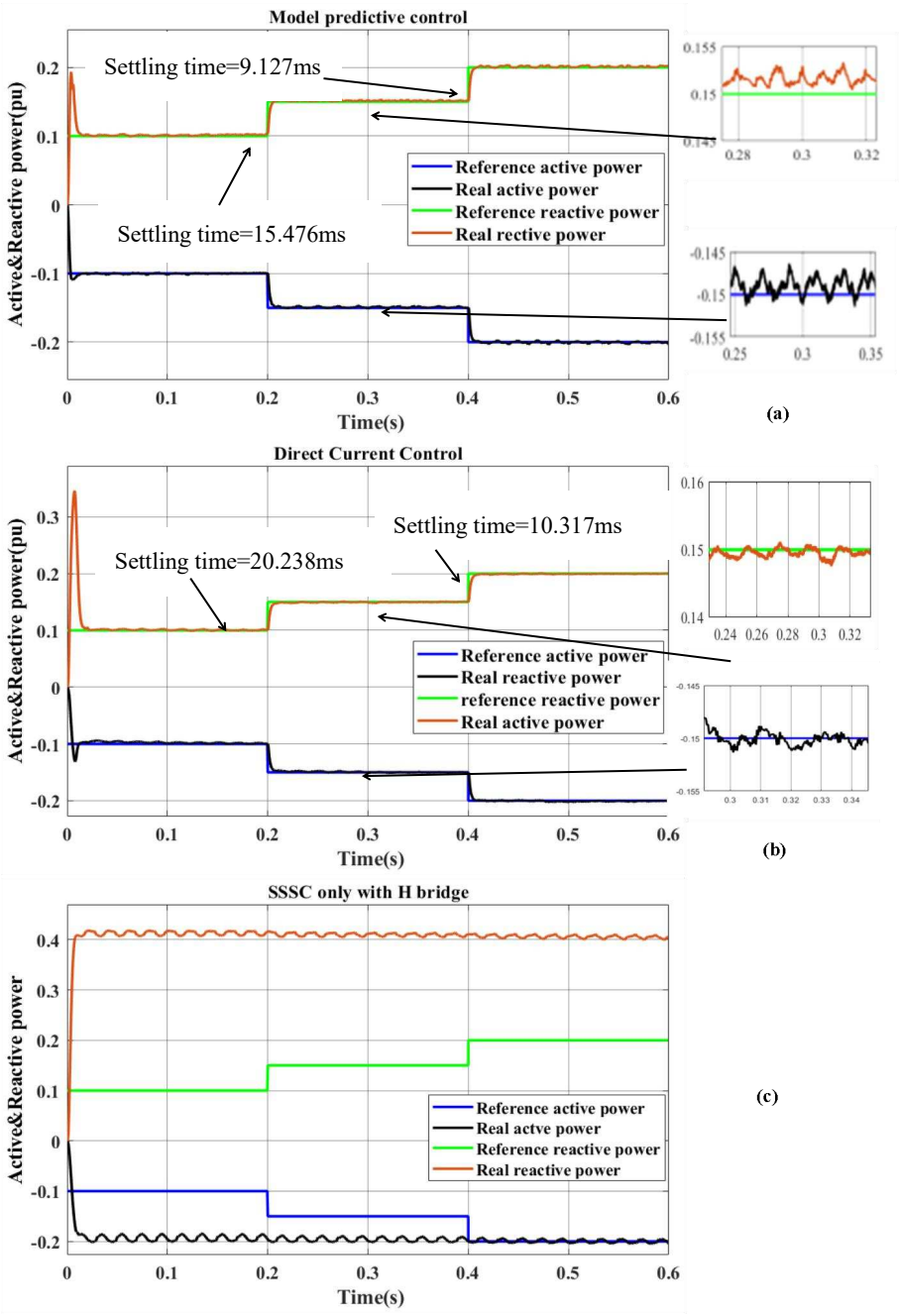

Fig.8 Powers measured from(a)model predictive current control(b)direct current control(c)only H-bridge in SSSC

The simulations are set to control the power flow through a transmission line with impedance R_L +jX_L at a voltage of 11kV. The direction from sending end to receiving end is set as positive.

The reference active power is varied from -0.1pu to -0.15pu at 0.2s and to -0.2pu at 0.4s. The reference reactive power is adjusted from 0.1pu to 0.15pu at 0.2s and changes to 0.2pu at 0.4s, so it is flowing from sending end to receiving end.

The power responses for model predictive current control and direct current control are shown in Figs.8(a) and (b). Fig.8(c) shows the result for SSSC with only the H-bridge and other parts the same. From Fig.8(c), SSSC with only the H-bridge cannot achieve power flow control because the DC voltage is too low for the SSSC to supply enough compensating voltage. Comparing figures (a) and (b) representing the two control methods used in BZSI-SSSC one can see that they can both achieve power flow control. The oscillations shown for direct current control are smoother and have less error than those for model predictive control. However, model predictive control has a lower settling time.

Conclusion

From Fig. 8(c), the SSSC with only the H-bridge cannot achieve power flow control because the DC voltage is too small for the SSSC to supply enough compensated voltage. Comparing figures (a) and (b), representing the two control methods used in the BZSI-SSSC shows that they can both achieve power flow control. The oscillation in current control can be better than with model predictive control. However, model predictive control can exhibit a shorter settling less time to settle down. Considering the stability and power loss of the system, the current control performs than the model predictive control. These results confirm the viability of the BZSI-SSSC, and its further advantages of a greater control range and bi-directional operation.

Reference

[1] Sen, K. (1998). SSSC-static synchronous series compensator: theory, modeling, and application. IEEE Transactions on Power Delivery, 13(1), 241 – 246.
[2] Kamarposhti, M., & Lesani, H. (2011). Effects of STATCOM, TCSC, SSSC and UPFC on static voltage stability. Electrical Engineering, 93(1), 33 – 42.
[3] Gajanayake, C., Vilathgamuwa, D., & Poh Chiang Loh. (2007). Development of a Comprehensive Model and a Multiloop Controller for Z-Source Inverter DG Systems. IEEE Transactions on Industrial Electronics, 54(4), 2352 – 2359.
[4] Rajakaruna, S., & Jayawickrama, L. (2010). Steady-State Analysis and Designing Impedance Network of Z-Source Inverters. IEEE Transactions on Industrial Electronics, 57(7), 2483 – 2491.
[5] Fang Zheng Peng. (2003). Z-source inverter. IEEE Transactions on Industry Applications, 39(2), 504 – 510.
[6] Husodo, B., Anwari, M., Ayob, S., & Taufik. (2010). Analysis and simulations of Z-source inverter control methods.2010 Conference Proceedings IPEC, 699–704.
[7] Huang, H., Zhang, L., & Chong, B. (2018). Control of A Modular Multilevel Cascaded Converter based Unified Power Flow Controller. IEEE.
[8]RODRIGUEZ J, CORTES P. Predictive control of power converters and electrical drives[M].US: John Wiley & Sons, Ltd, 2012.
[9]HU J, HE Y, XU L, et al. Predictive current control of grid connected voltage source converters during network unbalance[J]. IET Power Electronics, 2010, 3(5): 690-701.

Appendix

The coefficients for equation (9) and (10) are defined as:
$b_3=LL_LC;b_2=CLR_L;b_1=L_L(2D-1)^2+2L(1-D)^2;b_0=R_L(2D-1)^2;a_1=R_L(1-2D)(2U_C-U_{DC});a_2=L_LC(1-D);a_3=CR_L(1-D)+(1-D)^2;$